ABSTRACTS

POSTER SESSION 1

MONDAY 8TH, 17:30

SURFACE CHEMISTRY
CHEMICAL CHARACTERIZATION
ORGANIC FILMS
THIN METAL FILMS

Acknowledgments

The organizers and delegates of LEEMPEEM6 are very appreciative of the support given by the following institutions as well as the industrial sponsors and exhibitors:

Major Sponsors

ELMITEC	**Elmitec Elektronenmikroskopie GmbH** Albrecht-von-Groddeck-Str. 3 38678 Clausthal-Zellerfeld Germany **Phone:** +49 5323 1806 **Fax:** +49 5323 78932 **Email:** mail@elmitec.de **Web:** http://www.elmitec.de/
saes getters	**SAES Getters S.p.A.** Viale Italia 77 20020 Lainate (Milan) - Italy **Phone:** +39 02 93178 1 **Fax:** +39 02 93178 320 **Contact:** Mr. Paolo Manini Vacuum Systems Business Manager **Phone:** +39 02 93178284 **Email:** neg_technology@saes-group.com **Web:** www.saesgetters.com
SPECS®	**SPECS GmbH** Voltastrasse 5 D-13355 Berlin Germany **Phone:** +49 30 46 78 24 0 **Fax:** +49 30 46 42 08 3 **Email:** support@specs.de, sales@specs.de **Web:** http://www.specs.de/

Sponsors

	G. Gambetti Kenologia Srl Via Volta 27 20082 Binasco (Milano), Italy **Phone**: +39 02 90093082 **Fax:** +39 02 9052778 **Email**: sales@gambetti.it **Web:** http://www.gambetti.it/
	Omicron NanoTechnology GmbH Limburger Str. 75 65232 Taunusstein **Phone:** +49 6128 987 230 **Fax:** +49 6128 987 33 230 **Email:** info@omicron.de **Web:** http://www.omicron-instruments.com/
	Pfeiffer Vacuum Italia SpA Via San Martino, 44 20017 Rho, Milan, Italy **Phone:** +39 02 939905-23 **Fax:** +39 02 939905-33 **Email:** antonella.trentarossi@pfeiffer-vacuum.it **Web:** http://www.pfeiffer-vacuum.net/
	Photek Ltd 26 Castleham Road St Leonards on Sea East Sussex TN38 9NS United Kingdom **Phone:** +44 (0)1424 850555 **Fax:** +44 (0)1424 850051 **Email:** sales@photek.co.uk **Web:** http://www.photek.co.uk/
	Staib Instrumente GmbH HagenauStrasse 22, D-85416 Lagenbach, Germany **Phone:** +49 8761 76 240 **Fax:** +49 8761 76 24 60 **Email:** sales@staibinstruments.com **Web:** http://www.staibinstruments.com/

	Surface Preparation Laboratory Penningweg 69 F 1507 DE Zaandam The Netherlands **Phone:** +31-75-6120501 **Fax:** +31-75-6120491 **Email:** koper@surface-prep-lab.com **Web:** http://www.surface-prep-lab.com/
	Vacuum Science / VG Scienta Via G. Compagnoni, 37 20129 Milano **Phone:** +39 0239664549 **Email:** luca.rimoldi@vacuumscience.it **Web:** http://www.vgscienta.com/
	Vaqtec S.r.l. Cso V. Emanuele II 25/B 12100 Cuneo - Italy **Phone:** +39.0171.66507 **Fax:** +39.0171.64578 **Email:** info@vaqtec.com **Web:** http://www.vaqtec.com/
	Cinquepascal S.r.l. Via Carpaccio 35 20090 Trezzano sul Naviglio (Milano) Italy **Phone:** +39-02-4455-913 +39-02-4453-506 **Fax:** +39-02-4846-8659 **Email:** info@5pascal.it **Web:** www.5pascal.it

In-situ Observations of a desulfurization catalyst Ni$_2$P(0001) surface by photoemission electron microscopy

Takeshi Miyamoto[1], Hironobu Niimi[2], Makoto Kato[2], Shushi Suzuki[1], and Kiyotaka Asakura[1]

[1]*Catalysis Research Center and Department of Quantum Science and Engineering, Graduate School of Engineering, Hokkaido University, Kita21, Nishi10, Kita-ku, Sapporo, 001-0021, Japan*
[2]*JEOL Ltd., 3-1-2 Musashino, Akishima, Tokyo, 196-8858, Japan*

E-mail: mymt@cat.hokudai.ac.jp

Ni$_2$P shows an outstanding performance for hydrodesulfurization reaction from oil. The Ni$_2$P (0001) surface is a typical surface and has been characterized by several methods like LEED, STM, and theoretical calculations. It has two surface structures with different chemical composition of Ni$_3$P$_1$ and Ni$_3$P$_2$ as shown in Fig.1. Ni$_3$P$_2$ is thermodynamically stable. However, our previous STM measurement showed that the both surface structures coexisted on the Ni$_2$P(0001) at room temperature. However, the domain sizes were unknown because they were too large for STM measurement. DFT calculation indicated that the work functions are 5.22eV and 4.75eV, for Ni$_3$P$_2$ and Ni$_3$P$_1$ respectively. Thus, the domain sizes were measurable by PEEM. Here, we have investigated the domain sizes, their thermal stability and the adsorption properties of thiophene on both Ni$_2$P(0001) surface structures by PEEM and energy-filtered XPEEM.

Experiments were performed in a home-made energy-filtered X-ray photoemission electron microscopy (EXPEEM) system equipped with an original multipole Wien filter analyzer [1]. The sample was irradiated by using a high brilliance X-ray source with a rotating Al anode or a 200W Hg-Xe UV source with a low pass filter that cuts UV light higher than 5 eV in order to distinguish the two domains clearly. The Ni$_2$P(0001) surface was cleaned by cycles of Ar$^+$ bombardment and annealing at 753K. Surface cleanness was checked LEED and μ-XPS.

We distinguished both surface structures clearly by PEEM excited with 5 eV light. A bright and a dark area were assigned to the Ni$_3$P$_1$ and the Ni$_3$P$_2$ domain, respectively. During a heating process upto 573K, the Ni$_3$P$_1$ domain gradually disappeared around 530K and finally transformed to the Ni$_3$P$_2$ domain. We will discuss the chemical activity of the Ni$_2$P surface.

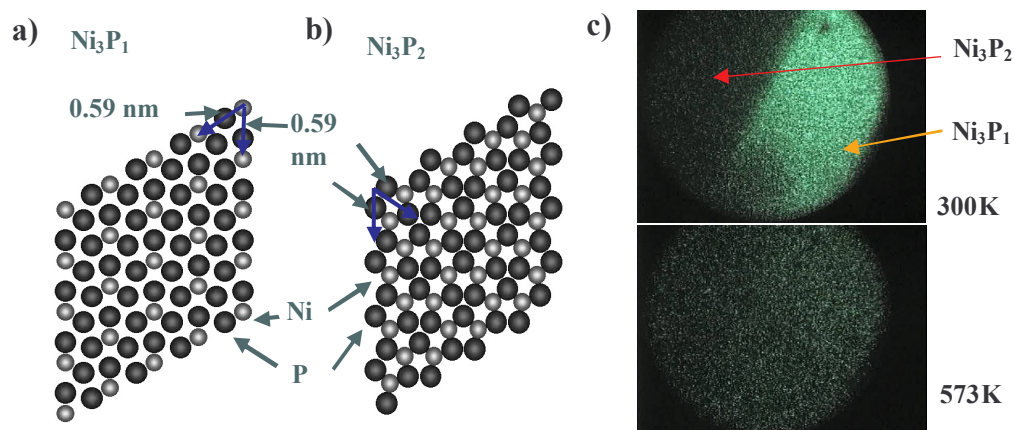**Figure 1a) and b):** Plane views of Ni$_3$P$_1$- and Ni$_3$P$_2$-terminated planes of the Ni$_2$P (0001) surfaces. They are repeatedly stacked with each other along the c-axis. c) The PEEM images of Ni$_2$P(0001) surface at 300K and 573K. The field of view for each image is 400μm. The areas of both domains were larger than 500×500 μm^2 at 300K.

References
[1] Niimi et al. Surf. Sci. 601 (2007) 4742

A comparative study in CCl$_4$ reaction on Ag/Si(111) surfaces: PEEM and PES investigations

Yunxi Yao, Qiang Fu, Xinhe Bao

State Key Laboratory of Catalysis, Dalian Institute of Chemical Physics, Chinese Academy of Sciences, Dalian 116023, P.R. China

E-mail: xhbao@dicp.ac.cn, qfu@dicp.ac.cn

We report a comparative study in the reactivity of bulk Ag(111), monolayer Ag film on Si(111), and Si(111)-7×7 surfaces via X-ray photoelectron spectroscopy (XPS), ultraviolet photoelectron spectroscopy (UPS), photoemission electron microscopy (PEEM), and scanning tunneling microscopy (STM). The monolayer Ag film grown on Si(111), which is known as √3×√3-Ag-Si surface structure, was obtained by depositing one monolayer Ag on the Si(111)-7×7 surface at 550 K. The most simple halogen methane, CCl$_4$, was chosen as the probe molecule to study the surface reactivity of the bulk Ag(111) surface, the monolayer Ag film, and the Si(111) surface. XPS and UPS data indicate that the monolayer Ag film presents unique reactivity to CCl$_4$ in comparison to the other two surfaces. For the PEEM study, a dedicated sample consisting of bulk Ag particles supported on the monolayer Ag film was prepared as shown in the schematics in Fig. 1. In situ PEEM imaging of the surface reaction in presence of CCl$_4$ shows a gradual change in the grey intensity from bright to totally dark on the Ag particles but little change on the √3×√3-Ag-Si surface. The grey intensity decrease is due to local work function increase from the dissociated Cl atoms. The experiments suggest that monolayer Ag is inert toward dissociation of CCl$_4$ compared to the Ag(111) and Si(111) surface. It has proposed that the confinement of 5sp electron of Ag atoms in the √3×√3-Ag-Si surface, which is delocalized in the bulk Ag(111) surface, is decisive to the different reactivity.
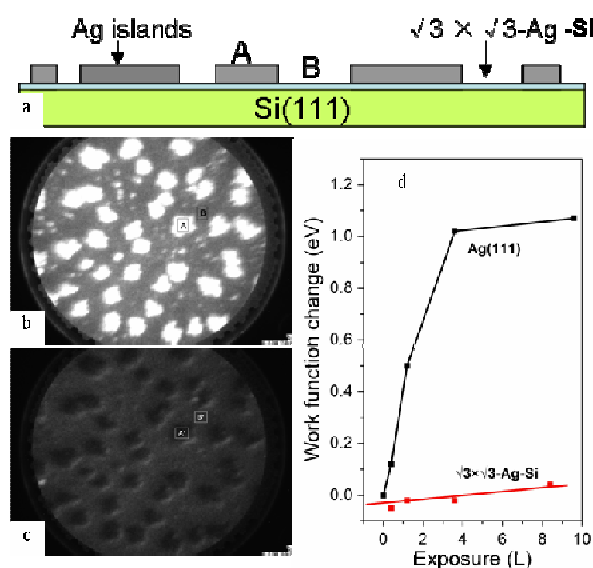
Figure 1: (a) Schematic representation of the √3×√3-Ag-Si surface supported Ag islands; (b) PEEM image of the Ag islands/√3×√3-Ag-Si sample before CCl$_4$ exposure. Field of view (FoV) is 27 μm; (c) PEEM image shows the same area in (b) but after 24 L (5.2×10^{-9} mbar × 6000 s) CCl$_4$ exposure; (d) the work function change (ΔΦ) of the Ag(111) and √3×√3-Ag-Si surfaces when exposed to different amount of CCl$_4$ at RT, measured from PES results.

References
[1] Y.X. Yao, X. Liu, Q. Fu, W.X. Li, D.L. Tan, X.H. Bao, ChemPhysChem 2008, 9: 975-979.

Bridging the complexity gap: surface specific screening of model Ir catalysts

Alix Cornish[1], Michael J. Gladys[2], Lars Thomsen[2], Tevfik O. Menteş[3], Miguel A. Niño[3], Lucia Aballe[3], Andrea Locatelli[3], Georg Held[1]

[1]*Department of Chemistry, University of Reading, UK*
[2]*School of Mathematical and Physical Sciences, University of Newcastle, Callaghan, NSW 2308, Australia*
[3]*Sincrotrone Trieste S.C.p.A., S.S. 14, km 163.5 in Area Science Park, 34012 Basovizza, Trieste, Italy*

Email: a.l.cornish@rdg.ac.uk, g.held@rdg.ac.uk

The 'complexity gap' is a major problem when data from single crystal surface science experiments are used in order to predict the properties of nanoparticles as they are found in industrial catalysts. Electronic and kinetic particle size effects, which are specific to small particles, as well as the chemistry of highly reactive edge or corner sites cannot be studied on single crystals. Polycrystalline surfaces offer a range of different, adjacent facets terminated by grain boundaries and can, thus, bridge this gap. Typical facet sizes range from several hundred nanometers to several hundred micrometers. LEEM and PEEM are the ideal tools to study the surface composition and morphology at this length scale.
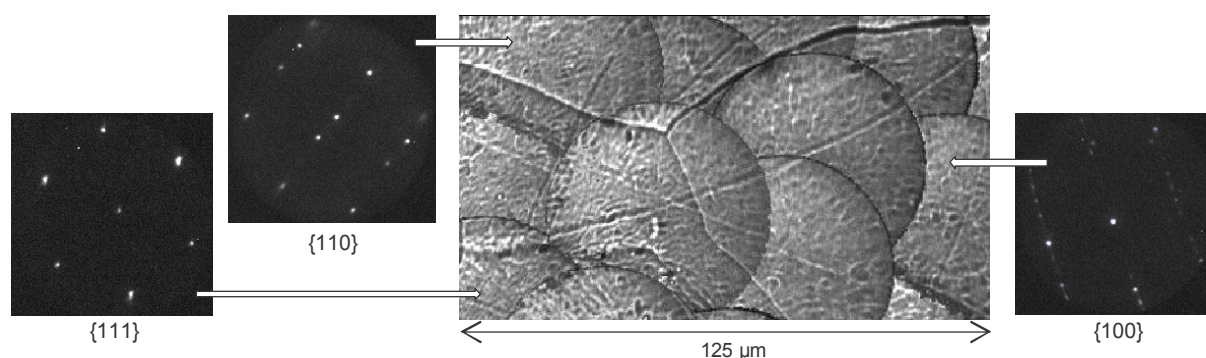

{110}

{111}

125 µm

{100}

Figure. Section of a LEEM (MEM mode) map of a polycrystalline Ir surface showing the boundaries between three facets which have been identified by their LEED patterns.

In this study we investigated the oxidation of CO on a polycrystalline Ir surface. Ir is a highly efficient catalyst for this reaction and has an important application in the field of automotive exhaust catalysts [1]. Work function (WF) studies on single crystal Ir{110} surfaces have shown that under constant oxygen pressure and increasing carbon dioxide pressure a decrease in WF occurs [2]. The maximum reaction rate occurs close to the WF maximum [2].

To model this reaction we measured the workfunction using the LEEM-MEM mode upon variations of the O_2 : CO pressure ratios (up to 10^{-6} mbar) for temperatures around 400 K. The local surface coverage of oxygen and carbon monoxide was monitored through the workfunction and X-PEEM spectra of the C1s peak. Using LEEM/PEEM, changes in these quantities could be recorded simultaneously and under identical conditions for several facets. The reactivity was found to increase in the order {311}<{110}<{100}<{111}. Significant deviation from Langmuir-Hinshelwood behaviour was observed, which indicates that in this pressure range the rate limiting step is adsorption rather than the surface reaction.

References
[1] V. Ponec, G. Bond, Catalysis by metals and alloys, Elsevier, Amsterdam, 1995.
[2] S. Ladis, S Kennou, N. Hartmann, R. Imbihl 1997 *Surface Science*, 382, 49.

Linking atomic to mesoscopic scale:
The Rh(110) surface oxide

C. Blasetti[1,2], C. Africh[1,2], F. Esch[2], G. Comelli[1,2,3],
T.O. Menteş[3], M.A. Niño[3], A. Locatelli[3]

[1]*Physics Dept. and CENMAT, University of Trieste, via Valerio 1, Trieste, Italy*
[2]*TASC-INFM-CNR Laboratory, Area Science Park, 34012, Trieste, Italy*
[3]*Sincrotrone Trieste S. C. p. A., Basovizza-Trieste 34012, Italy Italy*

Email: blasetti@tasc.infm.it

In previous studies we already characterized the structure of the surface oxide grown on Rh(110) by XPS, STM, LEED and DFT calculations [1]. The oxide has two rotational domains of mesoscopic dimensions that can hardly be studied by STM and that necessitate a mesoscopic technique.

By using LEEM in the darkfield mode, it was possible to unambiguously distinguish between the two domains and also to relate their relative proportion to the sample's history (see Fig.1a,b). On a clean surface, the crystal miscut dictates the surface oxide growth and hence also the prevailing domain. Moreover, we observe that after < 0.5 ML Au deposition on the pristine surface, the domains are fragmented and the reactivity upon hydrogen titration is dramatically decreased (Fig.1c).

As previously shown for the same system [2], the reactivity can be studied by LEEM/XPEEM down to nanometric resolution, giving complementary information with respect to STM measurements. We compare in the present study reactivities of a sub-monolayer oxide, of a complete, stoichiometric oxide and one of an oxide grown after sub-monolayer Au deposition (see Fig.1d).

In addition, LEED I(V) data collected from a single domain allow us to confirm that the surface oxide structure is consistent with that on Rh(100) [3].

a) 28eV,   b) 28eV,   c) 27.5eV,   d) 31eV,
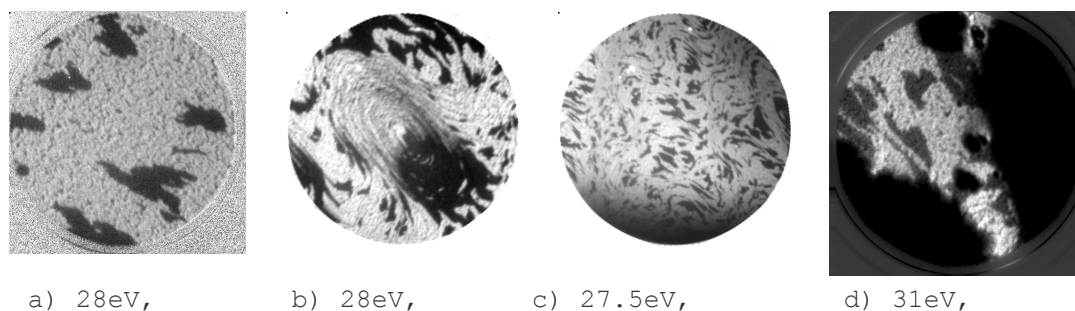
Figure 1. a) Darkfield image showing the two rotational domains of the surface oxide (dark and bright areas, resp.); b) mesa structure indicating how the domain distribution depends on the crystal miscut; c) fragmented oxide grown after <0.5 ML Au deposition; d) reaction front in the water formation on the stoichiometric oxide

References

[1] P. Dudin, A. Barinov, L. Gregoratti, M. Kiskinova, F. Esch, C. Dri, C. Africh and G. Comelli, *J. Phys. Chem.* **109** (2005) 13649; C. Dri, C. Africh, F. Esch, G. Comelli, O. Dubay, L. Köhler, F. Mittendorfer, G. Kresse, P. Dudin and M. Kiskinova, *J.Chem. Phys.* **125** (2006) 1.

[2] A.Locatelli, A.Barionv, L.Gregoratti, L.Aballe, S.Heun, M.Kiskinova, *J. Electr. Spectr. Relat. Phenom.* **144–147** (2005) 361.

[3] E. Lundgren, A. Mikkelsen, J.N. Andersen, G. Kresse, M. Schmid and P. Varga, *J. Phys. Cond. Matt.* **18** (2006) R481; K. Reuter and M. Scheffler, *Appl. Phys. A: Mater. Sci. Process.* **78** (2004) 793.

Vanadium oxide on W(110): An ultrathin model catalyst

B. Borkenhagen, G. Lilienkamp and W. Daum

Institut für Physik und Physikalische Technologien, Technische Universität Clausthal, Leibnizstr. 4, 38678 Clausthal-Zellerfeld, Germany

Email: B.Borkenhagen@pe.tu-clausthal.de

Ultrathin vanadium oxide films in the coverage range between submonolayer and several monolayers were epitaxially grown on W(110) by electron beam evaporation of vanadium in a controlled oxygen atmosphere. After subsequent heating under oxidizing or reducing conditions LEED reveals that ultrathin vanadium oxide flims can be grown in several superstructures, e.g. as (3x1), (2x1) or nearly hexagonal superstructures, the latter in Kurdjumov-Sachs orientation. The appearance of different superstructures appears to be specific for ultrathin vanadium oxide films as for thick films only a single surface structure has been reported [1]. By analysis of the respective Auger electron spectra, we are able to relate these superstructures to tungsten-vanadium surface alloys, tungsten oxides or vanadia in various oxidation states [2].

For superstructures with two domains, the dark field mode of LEEM was used to image individual domains and domain boundaries. In Fig. 1 the domains of a hexagonal vanadium oxide film are shown.
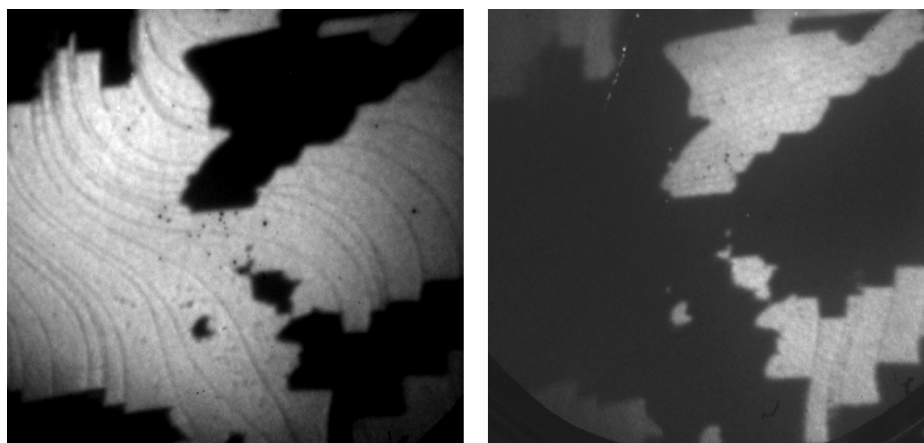

Fig 1. Dark field images of the two domains of a vanadium oxide film with hexagonal superstructure (E_{kin} = 4eV, FoV: 19µm x 19µm)

The dark field images show atomically flat terraces which are separated by monoatomic steps. The preferential alignment of the domain boundaries parallel and perpendicular to the steps is also evident. Comparison of the two images reveals that the substrate is completely covered with the vanadium oxide film. Several transitions between superstructures have been detected under defined temperature and oxygen partial pressure.

From our LEED, LEEM and AES results, we have compiled a preliminary diagram of the existence range of surface phases of vanadium and its oxides on W(110). In oxygen atmospheres the oxidation state of the vanadium can be increased up to values >3 at temperatures below 1000°C, while reducing atmospheres or electron impact lead to decreased oxidation states even at comparatively low temperatures.

References
[1] The A. C. Dupuis, "V2O3(0001)/Au111) and /W(110): Growth, Electronic Structure and Adsorption Properties", Dissertation, Humbold Universität Berlin (2002)
[2] C. N. R. Rao, D. D. Sarma and M. S. Hedge, Proc. R. Soc. Lond. A 370 (1980) 269-280

A LEED/LEEM investigation on phase transformations in ultrathin TiO$_x$/Pt(111) films

Stefano Agnoli[1], T. Onur Mentes,[2] Miguel A. Nino, [2] Andrea Locatelli[2] and Gaetano Granozzi, [1]

[1]*Department of Chemical Sciences, University of Padov, Italy*
[2]*Sincrotrone Trieste S.C.p.A., Basovizza-Trieste 34012, Italy*

Email: gaetano.granozzi@unipd.it

In recent years, we have managed to prepare and characterize several nanophases of TiO$_x$ on Pt(111) having rather different STM topography, stoichiometries and low energy electron diffraction (LEED) patterns [1] (see Figure 1). Adopting optimized recipes, almost pure nanophases were obtained and characterized, and theoretical models of their structures were reported [2].

Figure 1. Matrix notation of the LEED patterns of the different optimized TiO$_x$/Pt(111) nanophases organized according to the post-annealing oxygen pressure (P$_{O_2}$) [1b].

Exploiting the capability of the SPELEEM microscope at Elettra, we have used LEED and LEEM to follow the transformations among the different nanophases and to study the interplay between the different experimental parameters. Experiments were undertaken where the nanophase growth was monitored in *real time* by LEEM at different temperatures, oxygen pressures, and titanium coverages. It turns out that kinetic effects are rather important and that the actual transformations are strongly dependent on the actual deposition procedure.
In particular, the z→ z'→ rect transformations have been clearly observed. The formation in an oxidative ambient of the rect phase (i.e. a lepidocrocite-like nanosheet [2c]), has been morphologically examined in details, outlining the development of sharp wave fronts.

References

[1] (a) Sedona, F., Rizzi, G. A., Agnoli, S., Llabrés i Xamena, F. X., Papageorgiou, A., Ostermann, D., Sambi, M., Finetti, P., Schierbaum, K., Granozzi, G. *J. Phys. Chem. B* **2005**, *109*, 24411; (b) Finetti, P., Sedona, F., Rizzi, G. A., Mick, U., Sutara, F.,Svec, M., Matolin, V., Schierbaum, K., Granozzi, G. *J. Phys. Chem. C* **2007**, *111*, 869.
[2] (a) Barcaro, G. , Sedona, F., Fortunelli, A., Granozzi, G. *J. Phys. Chem. C* **2007**, *111*, 6095; (b) Sedona, F., Granozzi, G., Barcaro, G. ,Fortunelli, A., *Phys. Rev. B*, **2008**, *77*, 115417; (c) Zhang, Y., Giordano, L., Pacchioni, G., Vittadini, A., Sedona, F., Finetti, P., Granozzi, G. *Surf. Sci.* **2007**, *601*, 3488.

First-principles study of Au nanostructures on rutile TiO$_2$(110)

Adam Kiejna, Tomasz Pabisiak

Institute of Experimental Physics, University of Wrocław, Plac M. Borna 9, 50-204 Wrocław, Poland

Email: kiejna@ifd.uni.wroc.pl

Since the discovery of enhanced catalytic properties of dispersed gold nanoparticles on oxide supports [1] adsorption of metal atoms and formation of nanostructures on the oxide surfaces attracted a lot of interests. It is commonly agreed that the catalytic activity depends on the size of the gold particles, and on the oxide support. The catalytic activity of Au takes place at the perimeter of the nanoparticle [2], and the key factor is the presence of low coordinated Au atoms [3]. For the rutile TiO$_2$(110) surface it was demonstrated that the binding of Au to surface defects, like vacancies, is substantially stronger than to the stoichiometric surface. Recently, it has been proposed [4,5] that one-dimensional Au structures can be formed in a controlled manner, using ordered oxygen vacancies created on a TiO$_2$(110) surface during irradiation. The complemented first principles total-energy and electronic-structure calculations [4,5] demonstrated strong bonding of Au on TiO$_2$(110) bridging oxygen vacancies and formation of stable Au chains of monomer, dimer, and trimer type. It should be noted that the role of oxygen vacancies in the stabilization of Au particles on oxide surfaces under real reaction conditions has been debated [6].

In this work we examine the adsorption of small Au aggregates (atomic rows and clusters), of a size ranging from a monomer to a dozen of Au atoms per cell, on a partially reduced rutile TiO$_2$(110). The first principles calculations apply density-functional theory, plane wave basis, and projector augmented potential method. Our previous results [4,5] for monomer, dimer, and triple Au rows are extended to higher Au coverages and supplemented by results for clusters. The discussion is focused on the structure and bonding of one-dimensional Au rows on the missing row defected TiO$_2$(110) surface and their comparison with the respective properties of Au clusters adsorbed on the partially defected bridging O row. The calculations show the strong bonding to the substrate and the metallic nature of the Au rows. The work function of the Au/TiO$_2$(110) system is determined for different structures and coverages. We examine electron charge transfer and discuss the charging of clusters and its dependence on the cluster size. Results from this first-principles study give an insight into the nature of Au-Ti bond, the role of the amount of deposited metal on the observed electronic properties, and the growth behaviour of Au nanostructures on TiO$_2$(110).

References
[1] M. Haruta, N. Yamada, T. Kobayashi, S. Iijima 1989 *J. Catal.* 115, 301
[2] M. Haruta 2003 *Chem. Rec.* 3, 75
[3] T. Lopez, T. V. W. Janssens, B. S. Clausen et al 2004 *J. Catal.* 123, 232
[4] A. Locatelli, T. Pabisiak, A. Pavlovska et al 2007 *J. Phys.: Condens. Matter* 19, 082202
[5] T. O. Mentes, A. Locatelli, L. Aballe et al 2007 *Phys. Rev. B* 76, 155413
[6] D. Matthey, J. G. Wang, S. Wendt et al 2007 *Science* 315, 1692

SPELEEM observation of single molecular transition metal oxide nanosheets

Y. Kotani[1], T. Taniuchi[2], M. Osada[3], T. Sasaki[3], M. Kotsugi[4], F. Z. Guo[4], Y. Watanabe[4], M. Kubota[1] and K.Ono[1]

[1] *Institute of Materials Structure Science, High Energy Accelerator Research Organization (KEK) and Department of Materials Structure Science, The Graduate University for Advanced Studies, Tsukuba, Ibaraki 305-0801, Japan*
[2] *Institute for Solid State Physics, The University of Tokyo, Kashiwa, Chiba 277-8581, Japan*
[3] *International Center for Materials Nanoarchitechtronics and Nanoscale Materials Center, National Institute for Materials Science, Tsukuba, Ibaraki 305-0044, Japan*
[4] *SPring-8/JASRI, Kouto 1-1-1, Sayo, Hyogo 679-5198, Japan*

Email: kanta.ono@kek.jp

Recently there has been considerable interest in low-dimensional nanomaterials. Among them transition metal oxide nanosheet, that is derived from layered transition metal oxides by exfoliation, has attracted much attention, because of their unique property and low dimensionality. Co-doped $Ti_{0.8}Co_{0.2}O_2$ nanosheets show ferromagnetism at room temperature with giant magneto-optical effect in ultraviolet region [1,2]. For the device application and further material design, It is necessary to clarify the electronic structure of single molecular nanosheets and their interfaces.

In this study, we have investigated the electronic structure of a single molecular nanosheet $Ti_{0.8}Co_{0.2}O_2$ by x-ray nanospectroscopy using SPELEEM. Single molecular nanosheets were prepared by an LB method [3]. The local x-ray absorption and photoemission spectroscopy of the nanosheets were measured using SPELEEM with the spatial resolution of 85nm at BL17SU of the SPring-8. The chemical state of the Co atoms in the single molecular $Ti_{0.8}Co_{0.2}O_2$ nanosheets was found to be 2^+ low spin state from the local x-ray absorption and photoemission measurements. In addition, the different electronic structure was found in the nanosheet with different interface, indicating the existence of different charge transfer in the nanosheet interface. We also discuss the results of local electronic structure and charge transfer in single molecular (Ti, Co, Fe)O_2 nanosheets.
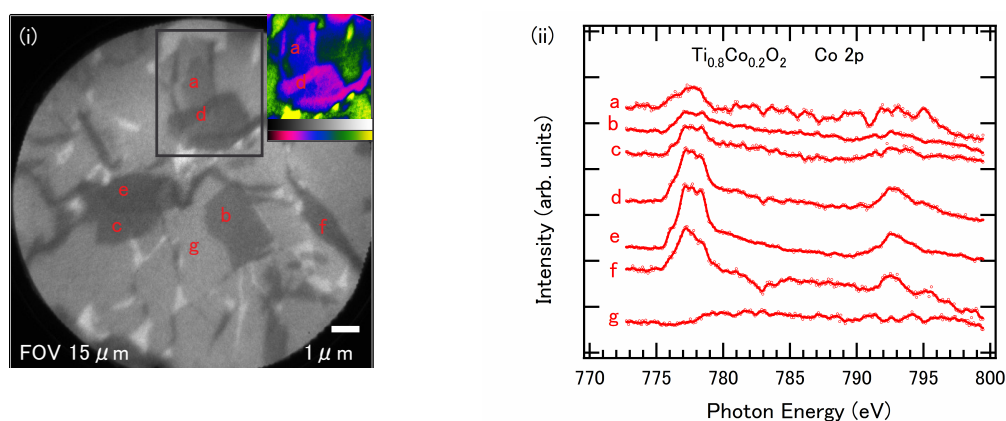
Figure. (i) PEEM images, and (ii) nano-XAFS spectra of $Ti_{0.8}Co_{0.2}O_2$ nanosheets on Au substrate.

References
[1] M. Osada, Y. Ebina, K. Fukuda, K. Ono, K. Takada, K. Yamaura, E.Takayama-Muromachi, T. Sasaki, *Phys. Rev.* B. **73**, 153301(2006).
[2] M. Osada, Y. Ebina, K. Takada, T. Sasaki, *Adv. Mater.* **18**, 295(2006).
[3] M. Muramatsu, K. Akatsuka, Y. Ebina, K. Wang, T. Sasaki, T. Ishida, K. Miyake and M. Haga, *Langmuir* **21**, 6590(2005).

Quantitative surface chemistry along a single nanowire: energy-filtered XPEEM of the metal catalyst diffusion

O. Renault[1], A. Bailly[1], P. Gentile[2], N. Pauc[2], T. Baron[3], L. –F. Zagonel[4], and N. Barrett[4]

[1]*CEA-LETI, MINATEC, 17, rue des Martyrs, 38054 Grenoble Cedex 09, France.*
[2]*CEA-DSM/INAC/SP2M/SiNaPS, 17 rue des Martyrs, 38054 Grenoble cedex 9, France.*
[3]*CNRS-LTM, UMR 5129, 17 rue des Martyrs, 38054 Grenoble cedex 9, France.*
[4]*CEA-DSM/IRAMIS/SPCSI, CEA Saclay, 91191 Gif-sur-Yvette, France.*

Email: orenault@cea.fr

Understanding and controlling the growth, usually performed by Vapour-Liquid-Solid method, of silicon nanowires from gold catalysts is crucial for optimized morphologies, surface and electronic properties of these nano-objects regarding their future applications. For the first time, we quantify at a mesoscopic scale the surface chemistry of single, tapered silicon nanowire (250-320 nm diameter as shown by SEM), using a novel X-ray photoelectron emission microscope with aberration-corrected energy-filtering (*NanoESCA*) and soft x-ray synchrotron illumination (ID08 beamline, ESRF, ~ 1.4×10^{10} ph.s^{-1}. 0.1% BW^{-1} at 700 eV within 25μm NanoESCA FoV). This spectromicroscope enables full-field, energy-filtered imaging using secondary, valence or core-level photoelectrons [1, 2]. With XPEEM we provide a direct, non-destructive chemical confirmation of gold migration along the sidewall surface as a result of tapering [3], from threshold and core-level photoemission nanospectra (200x200 nm^2). The presence of gold all along the sidewall is first evidenced by the Au4$f_{7/2}$ core-level image and corresponding nanospectra (Figure). From the Au4$f_{7/2}$ and Si 2p core-level local intensities weighed by the corresponding photoionization cross-sections, we have access to the partial coverage of gold on the nanowire sidewall (Figure). Gold has an evenly distributed island structure, covering 0.42±0.06 of the nanowire surface all along the wire length, corresponding to ~1.8 ML and in perfect agreement with the number of gold atoms lost by the catalyst during growth. The partial coverage of gold is further confirmed by a remarkable double-structure of the photoemission threshold in the local secondary electron distributions generated on the sidewall, and indicative of two distinct chemical phases present at the surface, the work function of which can be retrieved by modeling using Henke's functions [4]. Other examples of core-level XPEEM imaging of single nanowires dispersed on TiN substrates will be given, illustrating the sensitivity of the spectromicroscope used here.
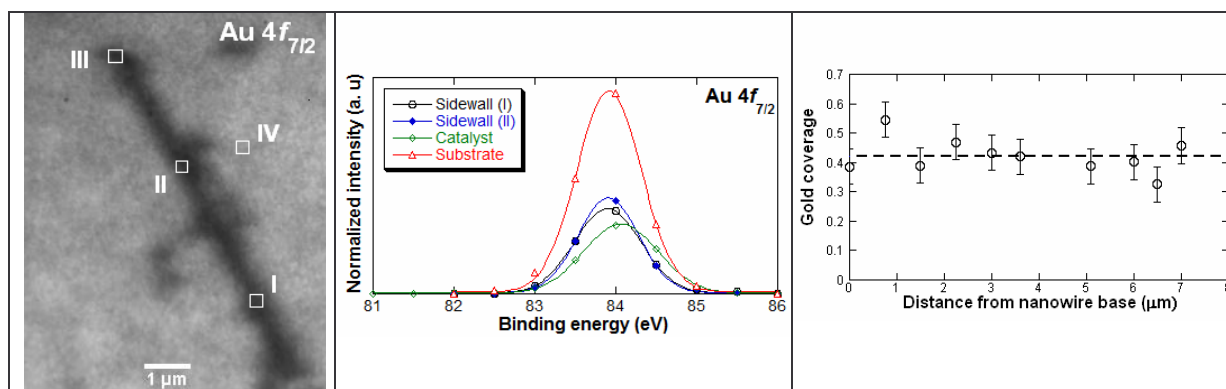
Figure. XPEEM Au4$f_{7/2}$ core-level image (left) and nanospectra (center). Right : Gold coverage along the nanowire sidewall derived from the Au4f and Si 2p local core-level intensities.

References

[1] M. Escher *et al.*, *J. Phys. : Cond. Matter* **17**, S1329 (2005).
[2] O. Renault *et al.*, *Surf. Sci.* **601** (2007), 4727.
[3] J. B. Hannon, S. Kodamka, F. M. Ross and R. M. Tromp, *Nature* **440**, 69-71 (2006).
[4] A. Bailly, O. Renault *et al.*, *Phys. Rev. Lett.* (submitted).

The Effect of Fe content on the Cu Activation of Sphalerite, (Zn,Fe)S, as determined by Scanning Photoelectron Microscopy

S.L. Harmer, D.A. Beattie, W.M. Skinner
[1]Ian Wark Research Institute, University of South Australia, Mawson Lakes, SA 5095

Email: Sarah.Harmer@unisa.edu.au

Sphalerite is the world's primary source of Zn and is commonly found in sulfide deposits with minerals such as pyrite, galena, quartz, calcite and chalcopyrite. Over seven million tonnes of Zn are extracted from zinc ores every year, where sphalerite is the principal component [1]. Separation of sphalerite from its associated sulfide minerals is commonly carried out by flotation using thiols attached to the Cu activated mineral surface. The mechanism of Cu ion adsorption on sphalerite surfaces has been the subject of controversy for a number of years [2-4]. The observed differences in the Cu activation of sphalerites have been compounded by the variability in composition of the mineral.

Sphalerite commonly forms with impurity elements including Fe, Cd, Mn, Cu and In replacing Zn on lattice sites. Concentrations can typically range up to 24 mol% for Fe, influencing both the band gap and reactivity of the mineral. This large variation in stoichiometry has a great effect on the processing of sphalerite ores. Improving our understanding of the surface chemical and physical properties of pure and impure minerals has become a target for enhancing the separation and extraction of base metals from their ores. To this end, the effect of surface morphology and bulk Fe concentration during Cu activation of sphalerite, have been investigated using SPEM.

Samples of nacia (14.79 wt% Fe) and santander (0.01 wt% Fe) sphalerite were cleaved along the (110) plane in 10^{-5} M $CuSO_4$ solution for 5 and 60 mins, at a pH of 5, prior to analysis using SPEM. Within the first 5 mins of reaction Cu had absorbed on the cleaved nacia surface preferentially to the low Fe Santander sphalerite. However, in each case the Cu adsorbed in the rough fractured regions of the surface rather than the (110) plane. The high Cu concentration was found to coincide with a higher concentration of polysulfides (Figure 1). After 60 min of reaction the Cu, Zn and Fe were quite uniformly distributed however the sulfur was concentrated at edges and rough fractured regions rather than the (110) cleavage surface. This study has provided a direct link between polysulfide formation and Cu adsorption has been made and the dramatic difference between the rate of Cu adsorption on high and low Fe containing sphalerites has been demonstrated.
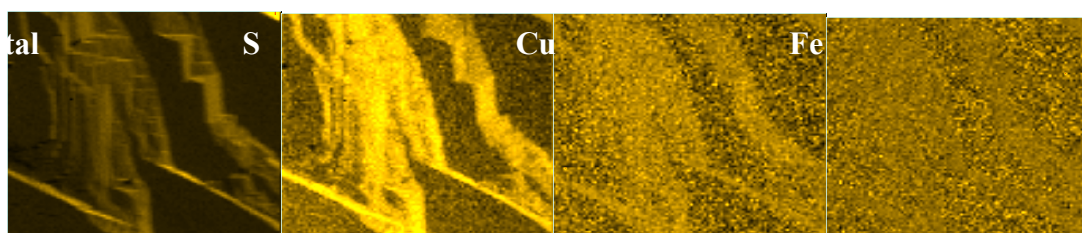
Figure 1: Total, S, S_n^{2-}, Cu and Fe SPEM images collected from a cleaved nacia sphalerite Cu activated at pH 5 for 5 mins.

References

[1] Dutrizac, J.E., Pratt, A.R. and Chen, T.T. 2003 *Met. and Mat. Process*: Principles and Technologies Vol III, 139.
[2] Buckley, A.N., Woods, R., and Wouterlood, H.J. 1989 *Int. J. of Min. Proc.* 26, 29.
[3] Kartio, I.J., Basilio, C.I., and Yoon, R.H. 1998 *Langmui*r 14, 5274.
[4] Ralston, J., and Healy, T.W. (1980) *Int. J Min. Process.* 7 (175-201), 203.

Surface orientation dependent termination and work-function of in situ annealed strontium titanate

L.F. Zagonel[1], N. Barrett[1,*], A. Bailly[2], O. Renault[2], M. Bäurer[3], M. Hoffmann[3], J. Leroy[1], S.-J. Shih[4], D. Cockayne[4]

[1]*CEA DSM/DRECAM/SPCSI, CEA Saclay, 91191 Gif sur Yvette, France*
[2]*CEA LETI Minatec, 17 rue des Martyrs, 38054 Grenoble cedex 9, France*
[3]*Institut für Keramik im Maschinenbau, Universität Karlsruhe, D-76131 Karlsruhe, Germany*
[4]*Department of Materials, Oxford University, Parks Road, Oxford OX1 3PH UK*

Email: nick.barrett@cea.fr

The surface chemistry of 1.2at.% Nb doped polycrystalline $SrTiO_3$ was studied by X-ray Photoemission Electron Microscopy (XPEEM) associated with soft x-ray synchrotron radiation. It is observed that grains can have different terminations as function of their orientation. Such chemical differences have an impact on the local work-function. The sample was sintered at 1700 K in a reducing atmosphere ($5\%H_2$+ $95\%N_2$) for 20 hours and annealed in vacuum at 1073 K for 3 hours in-situ. The photoemission electron microscope (PEEM) used is equipped with an α^2-aberration-corrected electron energy analyser which allows access to spatial resolutions of about 100 nm in full energy filtered images. [1,2] The electron energy analyser resolution was set to 550 meV. The same sample area was analysed by electron backscattering diffraction to determine the grain orientations.

The polycrystalline sample surface have been imaged at the Sr $3d_{5/2}$, Ti $2p_{3/2}$ and O $1s$ core levels. These images show that annealing created some preferential surface termination correlated to the grain orientation.[3] The impact of such termination can be observed indirectly as differences in the local surface work-function. Figure 1 (a) shows an image recorded using secondary electrons at an energy of 3.85eV. Darker grains have a higher work-function than brighter grains. A sequence of images was recorded for kinetic energies in the range of 2 to 10 eV. From this image sequence, spatially resolved spectra can be extracted. The local work-function of each grain is determined by fitting an error function to the spectra extracted from the grain area. Figure 1(b) shows a histogram of the number of grains observed for a given work-function (a total of 60 grains were analysed). The average value is 4.2 eV with a ~0.1 eV dispersion.[4] These work-function values are also related to the grain orientation. In figure 1(c) the work-function is plotted as function of the grain orientation. The [100] oriented grains have a lower work-function with respect to those oriented [101] or [111]. These results show that depending on the surface orientation and termination, the Nb doped $SrTiO_3$ can display work-functions ranging from 4.0 to 4.3 eV. Since the work-function affects real device performance, this approach may be extremely interesting for many technologically important surfaces.

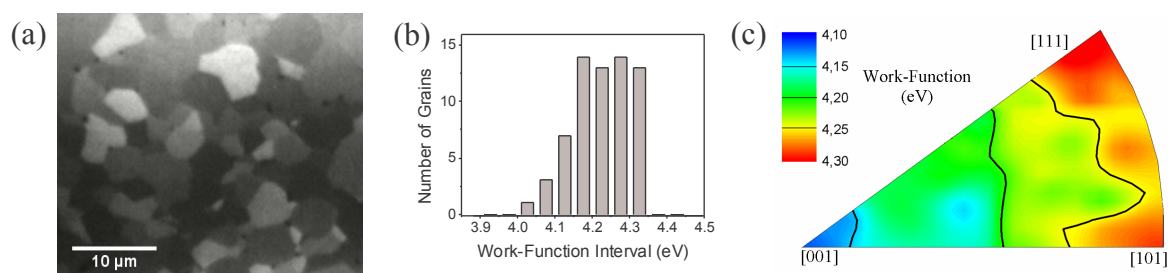**Figure 1.** (a) Secondary electrons at a kinetic energy of 3.85 eV. (b) Histogram of work-functions of measured grains. (c) Averaged dependence of work-function on grain orientation.

References
[1] M. Escher *et al.*, *J. Phys.: Condens. Matter* **17** (2005) S1329.
[2] O. Renault *et al.*, Surf. Sci. 601 (2007) 4727.
[3] L. F. Zagonel *et al*, Surf. Sci. 2008.
[4] D. Vlachos, *et al*, Surface Science **550**, 213 (2004).

Addressing the Surface Properties of Individual 1-D SnO$_2$ Nanostructures

A. Kolmakov[1], S. Potluri[1],

A. Barinov[2] , T. O. Menteş[2], L. Gregoratti[2], M. A.Niño [2], A. Locatelli[2], M. Kiskinova[2]

[1] *Southern Illinois University at Carbondale, USA; E-mail: akolmakov@physics.siu.edu*
[2] *Sincrotrone Trieste S. C. p. A., Basovizza-Trieste 34012, Italy*

Email: akolmakov@physics.siu.edu

Understanding size/dimensionality dependent phenomena and processes relevant to chemical sensing and catalysis require analytical methods with high *surface* sensitivity, which can exploit the structure and composition of nano-materials at their natural length scales and working conditions [1]. In the present study we explored the potentials and complementary capabilities of X-PEEM and LEEM to shed light on the properties of individual SnO$_2$ nanowires and nanobelts. Our results demonstrate the unique opportunities provided by synchrotron-based spectromicroscopy for structural and chemical analysis, including *in-situ* characterization of electron transport properties of a nanostructure wired as an active element in chemiresistor devices [2]. Few experimental challenges and their solutions will be discussed.
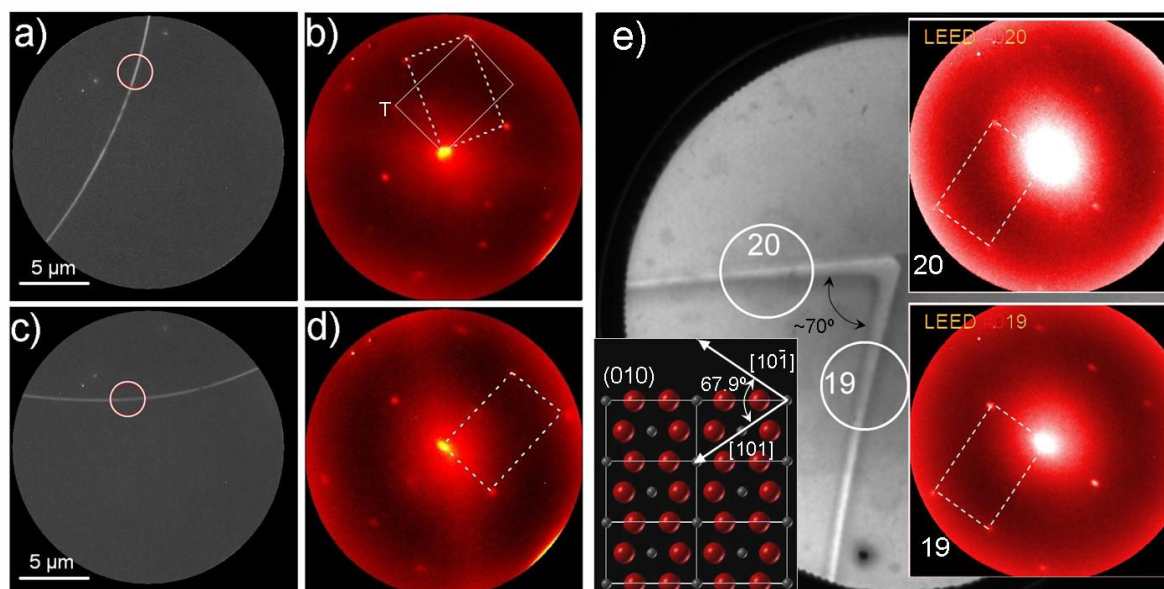
Figure   (a, c) Two LEEM images (FOV 20 µm) and corresponding (1x1) LEED patterns (b, d) collected from the two areas (marked with red circles) along the individual nanostructure. The rotation of the (1x1) LEED patterns approximately follows the bending of the nanostructure in real space. e) LEEM (FOV 6 µm) image of the "kinked" nanostructure and (1x1) LEED patterns collected from different "arms". In spite of the changed orientation in the real space the surface structure and its orientation is preserved along the length of the nanostructure. The inert depicts the model of the (010) facet and crystallographically equivalent growth directions.

References
[1] A. Kolmakov, U. Lanke, R. Karam, et al 2006 *Nanotechnology*, 17, 4014
[2] A. Kolmakov, S. Potluri, A. Barinov, T. O. Mentes et al (to be submitted)

Grain boundary phases in Austenitic stainless steels: Quantitative elemental composition studies by X-ray photoemission electron microscopy

B. M. Haines, U. D. Lanke and S. G. Urquhart
Department of Chemistry, University of Saskatchewan, Saskatoon, SK, S7N 5C9, Canada

Email: Stephen.Urquhart@usask.ca

Embrittlement and liquidation cracking of stainless steel alloys used in high temperature applications are a serious materials problem in the petrochemical industry. A first step in tackling such embrittlement problems is developing an understanding of embrittlement mechanisms, from which appropriate metallurgical solutions may follow. We have used x-ray photoelectron emission microscopy (X-PEEM) as an analytical microscopy to examine the microstructure and grain boundary chemistry in stainless steel alloys prone to liquidation cracking. Sensitivity to the elemental composition and chemical state of grain boundary phases is obtained through Near Edge X-ray Absorption Fine Structure (NEXAFS) spectroscopy. We use NEXAFS spectroscopy in the X-PEEM microscope to perform quantitative elemental composition measurements at spatial scales (<100 nm) that are difficult to access by traditional SEM-EDX methods. Quantization of model alloys demonstrated an uncertainty of approximately 2 percent. With the addition of an imaging energy filter, XPS mapping can also be performed; here we find a significant increase in sensitivity to dilute elements, such as carbon and silicon, over NEXAFS spectroscopy. Through a combination of NEXAFS and XPS spectromicroscopy studies in X-PEEM, we have identified a eutectic phase believed to be responsible for the embrittlement of type HP45 stainless steel alloys.

Chemical mapping of phase-separated organic nanostructures studied by X-ray photoemission electron microscopy

S. Christensen, B. M. Haines, U. D. Lanke, S. E. Qaqish, M. F. Paige and S. G. Urquhart
Department of Chemistry, University of Saskatchewan, Saskatoon, SK, S7N 5C9, Canada

Email: Stephen.Urquhart@usask.ca

The structure and composition of phase-separated arachidic acid ($C_{19}H_{39}COOH$, AA) and perfluorotetradecanoic acid ($C_{13}F_{27}COOH$, PA) Langmuir-Blodgett (LB) monolayer films were characterized using a combination of x-ray photoelectron emission microscopy (X-PEEM), electron-energy resolved secondary electron emission microscopy (SEEM) and atomic force microscopy (AFM). X-PEEM provides composition information with high lateral spatial resolution through the chemical sensitivity of NEXAFS spectroscopy; SEEM provides sensitive yet indirect structural and electronic sensitivity, while AFM provides high resolution imaging, both in terms of lateral and vertical film topography. SEEM is a new analytical capability realized through the imaging energy filter on the Canadian Photoemission Electron Research Spectromicroscope (Elmitec PEEM3) located at the Canadian Light Source. Studies of well characterized LB thin films are ideal for understanding the sensitivity of SEEM imaging, particularly for organic nanostructures. In this presentation, from NEXAFS and AFM results, we understand that the discontinuous domains are enriched in AA while the surrounding continuous domains are a mixture of both AA and PA.
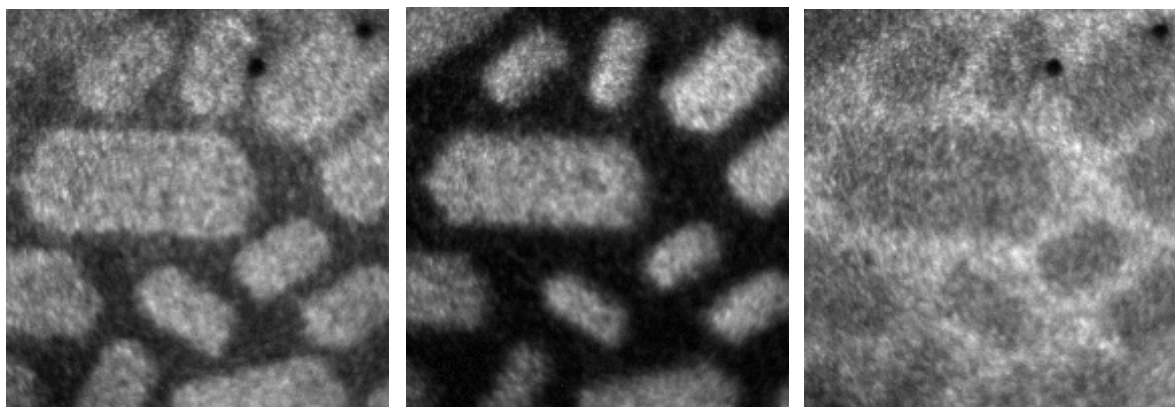
.

Figure SEEM images recorded for a phase separated LB monolayer, with a relative electron kinetic energy of -0.5 eV (left), 0 eV (centre) and +0.5 eV (right).

References

[1] S. Christensen, U.D. Lanke, B. Haines, S.E. Qaqish, M.F. Paige and S.G. Urquhart, Journal of Electron Spectroscopy and Related Phenomena **162** (107) 2008.

From interfaces to surfaces: Soft X-ray spectromicroscopy investigations of diindenoperylene thin films on gold

M. B. Casu, T. Chassé

Institute of Physical and Theoretical Chemistry, University of Tuebingen, Auf der Morgenstelle 8, 72076 Tübingen, Germany

Email: benedetta.casu@uni-tuebingen.de

Nowadays organic electronic devices are widely present on the market; however, to favour further technical developments, the full understanding of electronic, structural, and morphological properties of organic materials plays a paramount role. Diindenoperylene (DIP, $C_{32}H_{16}$) is a perylene-based molecule that shows a very high hole mobility already in thin films [1], good film forming properties, and thermal stability. It may be considered as a promising molecule for electronics [2].

In this work we present the results of photoemission electron microscopy (PEEM), scanning transmission X-ray microscopy (STXM), X-ray photoemission (XPS), and near-edge X-ray absorption fine structure (NEXAFS) spectroscopy investigations (all taken at the C 1s edge) on DIP thin films deposited on polycrystalline gold. We focused on the different molecular orientations that may occur while growing a film, from the interface with the substrate to the surface. PEEM and XPS reveal the occurrence of Stranski-Krastranov growth modes. STXM images together with nano near-edge X-ray absorption fine structure spectra show that different electronic structure domains occur depending on different sample thicknesses. Based on the synergy of our results, we propose a model for the growth of DIP thin film deposited with a relative low deposition rate (0.3 nm/min) on gold (polycrystalline and single crystal).
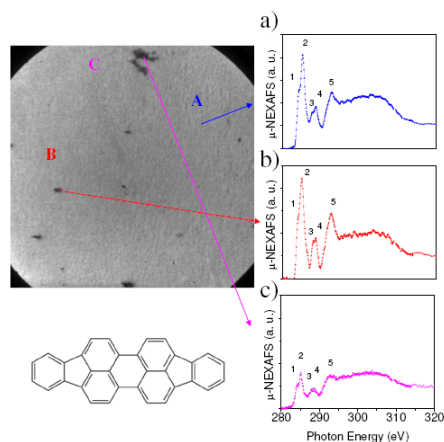
Figure 1 PEEM stack, for a 12 nm thick film, integrated in the photon energy range between 280 and 320 eV, together with the μ-NEXAFS spectra (a, b and c) for three representative regions as indicated. The μ-NEXAFS spectra have the same scale to facilitate the comparison. The DIP molecular structure is also shown.

References
[1] Karl N., Synth. Met. 133-134, 649 (2003).
[2] Dürr A. C., Schreiber F., Kelsch M., Carstanjen H. D., Dosch H., Adv. Mater. 14, 961 (2002).

Epitaxially grown pentacene on the h-BN/Rh(111) nanomesh

A.A. Zakharov[1], A.B. Preobrajenski[1], M.L. Ng[1,2], A.S. Vinogradov[3] and N. Mårtensson[1, 2]

[1] *MAX-lab, Lund University, Box 118, 22100 Lund, Sweden*
[2] *Department of Physics, Uppsala University, Box 530, 75121 Uppsala, Sweden*
[3] *Institute of Physics, St.-Petersburg State University, 198504 St.-Petersburg, Russia*

E-mail: Alexei.Zakharov@maxlab.lu.se

Pentacene (Pn - $C_{22}H_{14}$) is a promising organic molecule since it has been successfully used in the organic field-effect transistors having field-effect mobility surpassing that of amorphous silicon [1-2]. However, the very first challenge in realizing the concept of pentacene organic thin film transistor is to find a substrate suitable for long range epitaxial growth of structurally perfect pentacene [3]. Furthermore, it is crucial to determine the molecule orientation and structural quality for optimization of its functionality and possibly, to further functionalize/decorate it with other molecules.

In this contribution we report the outcome of our investigation on the possibility and feasibility of growing pentacene via thermal evaporation on h-BN/Rh(111) at RT. This substrate is supposed to be chemically inert and electrically insulating. Besides, it is periodically corrugated with a period of just ~3 nm, thus being promising for an epitaxial growth of pentacene. For the first monolayer (ML), pentacene grows in the layer-by-layer mode forming large islands (Fig., left) until a complete wetting layer is formed. The molecules are ordered very well, as can be judged from the micro-LEED images. Within one large island they form several (up to six) domain types with different orientation relative to the substrate.
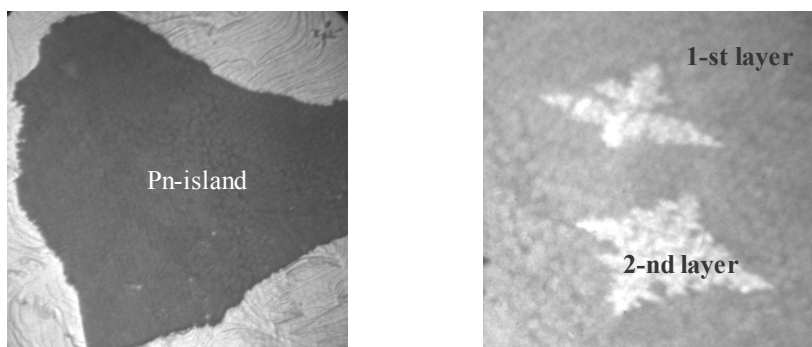

Figure. LEEM images from a sub-ML pentacene (left) and 1.3ML pentacene (right) on h-BN/Rh(111). FoV=15μm, E=3.5eV (left) and 5.1eV (right).

Above the first ML the molecules start to assemble in fractal islands instead, with the island size growing for elevated substrate temperature upon deposition (Fig., right). On the other hand, pentacene does not grow in islands on clean Rh(111) but it adsorbs directly on the spots where it falls due to stronger chemical bonding, as can be judged from C 1s NEXAFS and core-level PES. In addition, core-level PES measurements show that these molecules are chemisorbed on Rh but only physisorbed on the nanomesh.

References
[1] N. Koch, ChemPhysChem **2007**, 8, 1438-1455.
[2] C. D. Dimitrakopoulos, J. Appl. Phys. 1996, **80** (4), 2501.
[3] H.-K. Lee et. al., Surf. Sci. 601 (2007) 1456-1460.

Real-Time Observation of PTCDA Growth on Ag(111) - a SMART Investigation

Florian C. Maier[1], Pierre L. Levesque[2], Thomas Schmidt[1,2], Helder Marchetto[2], Ulrich Groh[1], Tomas Skala[2], Rainer Fink[3], Hans-Joachim Freund[2] and Eberhard Umbach[1,4]

[1] *Universität Würzburg, Experimentelle Physik II, 97074 Würzburg*
[2] *Fritz-Haber-Institut der Max-Planck-Gesellschaft, 14159 Berlin*
[3] *Univ. Erlangen-Nürnberg, Phys. Chemie II, 91058 Germany*
[4] *Forschungszentrum Karlsruhe, 76021 Karlsruhe*

Email: Florian.Maier@physik.uni-wuezrburg.de

The spectro-microscope SMART [1], the aberration corrected high resolution LEEM/PEEM system, has been used in its final version to investigate the growth of thin organic films on metal substrates and their interaction.

The growth of PTCDA (3,4,9,10 perylene-tetracarboxylic-acid dianhydrid) on a single-crystalline Ag(111) surface has been observed *in-situ* and in *real-time* at substrate temperatures between 210 K and 380 K. LEEM, PEEM and LEED studies reveal the dependence of the growth mode, the structure and the phase formation on both, the temperature and the substrate morphology [2].

Above room temperature PTCDA grows in the Stranski-Krastanov mode (i.e. a bi-layer followed by 3D islands), whereas at medium temperatures a closed organic film in a mound like quasi layer-by-layer fashion is formed. However, at low temperatures (below 250 K) growth in Vollmer-Weber fashion has been observed, meaning that organic layers do not close anymore but isolated pyramid-like shaped 3D islands start growing directly on the substrate, giving insight into the kinetics of the flat molecules diffusing on the silver and PTCDA surface.

The formation of different structural phases will be shown and details of the *real-time* investigation like the kinetic behaviour of the growing layers, the metastability and desorption of single layers will be discussed.
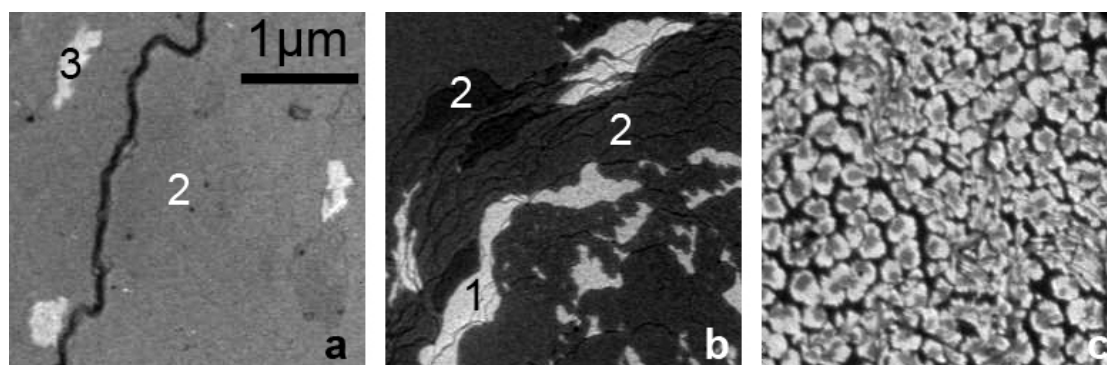
Figure. Three LEEM images with 2.7eV start voltage show different growth modes of PTCDA on Ag(111) at different sample temperatures: (a) 380 K, (b) 290 K and (c) 210 K. Stranski-Krastanov growth is seen in (a) where layer 1 and 2 are closed completely before layer 3 starts. While the rightmost image (c) shows Vollmer-Weber growth where black corresponds to the Ag(111) substrate, the light grey to the 1st and the dark grey to the 2nd layer. Image (b) shows the bright 1st layer and on top two phases of the 2nd layer.

References
[1] R. Fink et al., J. Electr. Spectrosc. Rel. Phen. **84**, 231 (1997)
[2] Marchetto et al., Chem Phys **325**, 178 (2006)

The growth mechanism of pentacene on HOPG

H.W. Liu[1], A. Al-Mahboob[1], Y. Fujikawa[2], T. Hitosugi[1], T. Hashizume[1], T. Sakurai[1], Q.K. Xue[1,3]

[1]WPI-Advanced Institute for Materials Research, Tohoku University, Sendai 980-8577 Japan
[2]Institute for Materials Research, Tohoku University, Sendai 980-8577 Japan
[3]Department of Physics, Thsinghua University, Beijing 100084, China

Email: liu@wpi-aimr.tohoku.ac.jp

Pentacene ($C_{22}H_{14}$) has been received significant attention because of its best thin-film FET performance among organics. The electrical properties of OFET are affected by the molecular orientation/packing in domain. The LEEM of Pn/aromatic hydrocarbons system like Pn/C_{60} showed a competitive growth between Pn having standing-up molecule orientation and a lying-down orientation [1]. A simple Pn/carbon-uppermost system such as Pn/HOPG has been studied by PEEM, and its growth mechanism was speculated by the UPS spectra [2].

Here we investigated growth of Pn/HOPG by real time LEEM. The LEEM image and the diffraction patterns in Fig. 1 show that (i) A 6-fold ordered wetting layer of Pn with lying-down molecular orientation (dark contrast in Fig. 1a) is formed on HOPG. We didn't observe the wetting layer growth as there is no contrast in LEEM image. Its existence can be confirmed by LEED. (ii) On the top of wetting layer, subsequently, the nucleation of lying-down phase and a delayed nucleation of standing up phase have been observed. (iii) The recorded LEED patterns indicate the symmetric structure of the wetting layer, and asymmetric surface lattice of the lying-down Pn islands, which might be associated with tilted Buddha-lying orientation during the growing.
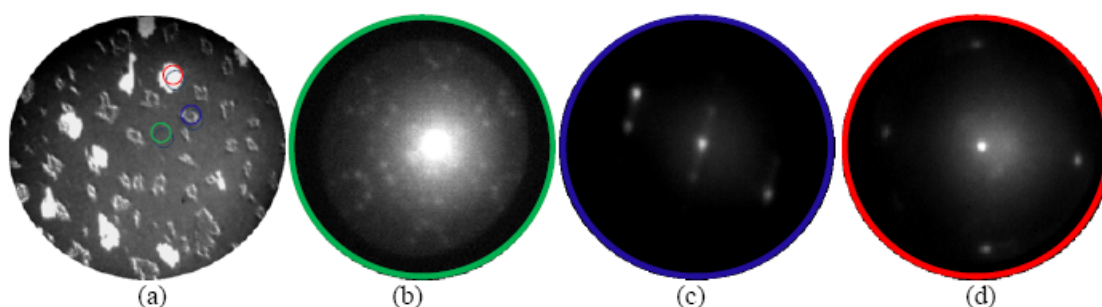
Figure 1. (a) LEEM image of Pn on HOPG at room temperature. (b)-(d) LEED patterns recorded from the areas in (a) marked as green, blue and red circles, respectively. (b) a pattern from a 6-fold ordered lying down wetting layer; (c) an asymmetric pattern from a lying-down Pn island; (d) a pattern from a standing up Pn island.

References
[1] A. Al-Mahboob *et al.* (unpublished)
[2] M. Shionoiri, M. Kozasa, S. Kera, K. Okudairai, and N. Ueno, *2007 Jpn. J. Appl. Phys.*, 46, 1625

Graphene formation on annealed SiC

John Boeckl[1], Larry Grazulis[1], William Mitchell[1], Migel Angel Niño[2], T.Onur Menteş[2], Andrea Locatelli[2]

[1]*Air Force Research Laboratory, Materials and Manufacturing Directorate, WPAFB, Dayton, OH 45433-7707, USA*

[2]*Sincrotrone Trieste SCpA, SS 14, km 163.5 in Area Science Park, 34012 Basovizza, Trieste, Italy*

Email: john.boeckl@wpafb.af.mil

Epitaxial graphene on SiC(0001) is receiving interest for studying both relativistic quantum physics and producing next generation electronic device structures. We have previously reported on the formation of nano-carbon structures during high temperature (1400°C–1800°C) moderate vacuum (10^{-2}–10^{-5} torr) surface decompositions of SiC (0001) [1,2]. With precise control of this thermal decomposition process the formation of an epitaxial graphene layer can result [3-5]. It has also been shown that low energy electron microscopy (LEEM) imaging can be used to determine the layer thickness of graphene formed under such annealing conditions [4]. Although the process is thought to occur via the sublimation of Si leaving a C-rich surface that converts to sp^2-hybridized graphite, this transformation is not fully understood. In order to reveal the evolving surface morphology, *in situ* e-beam sample heating and real time LEED imaging were used to monitor the progressive formation of crystalline graphite on 6H-SiC (0001) surfaces. Corresponding LEEM and X-Ray Photoemission Electron Microscopy (XPEEM) snapshots were obtained as each crystallographic reconstruction providing direct insight into the surface chemistry and morphology as the transition occurred.

Ex situ characterization of the samples by RAMAN spectroscopy, atomic force microscopy (AFM), and transmission electron microscopy (TEM) have confirmed the presence of graphene on the SIC substrate. Figure 1 provides the evidence for the formation of graphene. Figure 1(a) shows the LEEM image as the graphene film was initiated. Figure 1(b) shows an AFM scan of the sample after it was removed from the LEEM system. Figure 1 (c) is a RAMAN spectrum for this material clearly showing the second order D band peak of bi-layer graphene.
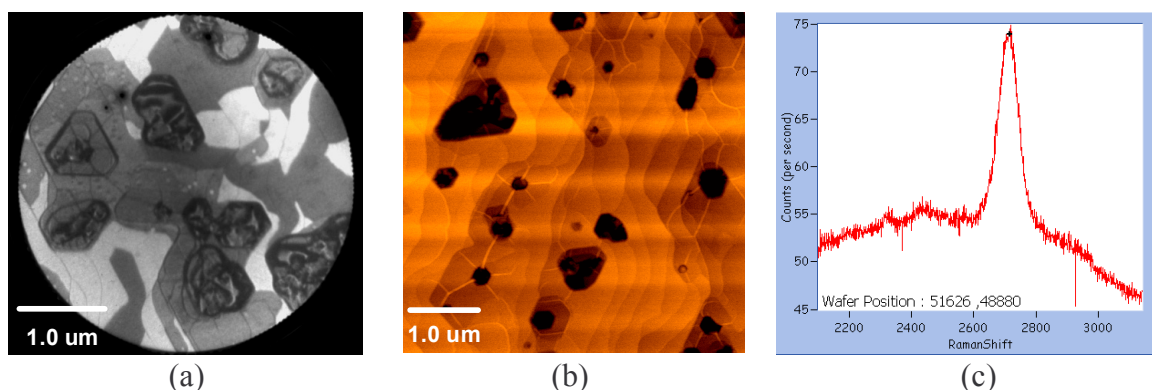

(a)   (b)   (c)

Figure 1. (a) LEEM image of a graphene film on a SiC (0001), recorded with an electron energy of Evac + 4.85 eV and 4 um field of view, (b) AFM image of the resulting film, (c) RAMAN spectrum of the 2D peak demonstrating bi-layer graphene.

References
[1] J. Boeckl, W. C. Mitchel, J. Rigueur, W. Lu, *Mater. Sci. Forum* **527-529***, 1579-1582 (2006).
[2] J. Harrison, S. N. Sambandam, J. J. Boeckl, et al, *J. Appl. Phys*. **101**, 104311 (2007).
[3] I. Forbeaux, J.-M. Themlin, and J.-M. Debever, *Phys. Rev. B* **58**, 16396 - 16406 (1998).
[4] T. Ohta, F. El Gabalay, A. Bostwick, et al, *New J. Phys*. **10,** 023034 (2008).
[5] M. Kusunoki, J. Shibata, M. Rokkaku, et al, *Jpn. J. Appl. Phys*. **37**, L605 (1998).

Morphology and structure of graphene films and the interface layer on SiC

Taisuke Ohta[1], Gary L. Kellogg[1], Farid El Gabaly[2], Konstantin V. Emtsev[3],
Aaron Bostwick[2], Jessica L. McChesney[2,4], Andreas K. Schmid[2], Thomas Seyller[3],
Karsten Horn[4], Eli Rotenberg[2]

[1]*Sandia National Laboratories, Albuquerque, New Mexico 87185, USA*
[2]*Lawrence Berkeley National Laboratory, Berkeley, California 94720, USA*
[3]*Lehrstuhl für Technische Physik, Universität Erlangen-Nürnberg, 91058 Erlangen, Germany*
[4]*Fritz-Haber-Institut der Max-Planck-Gesellschaft, 14195 Berlin, Germany*

Email: tohta@sandia.gov

Graphene, a hexagonal crystalline layer of carbon with charge carriers of extraordinary high mobility ($>200{,}000$ cm^2/V·sec) and unique Dirac fermion characteristics, holds great promise for ultra high-speed, low-power and coherent nano-electronics [1]. To realize graphene-based electronics, techniques must be developed to reproducibly synthesize high quality graphene onto technologically-relevant substrates over large areas, which is difficult without a fundamental understanding of graphene formation. Here we study the emerging morphology and the interface structure of epitaxial graphene films on (0001)-oriented silicon-carbide (SiC) substrate using low energy electron microscopy (LEEM) [2] as well as angle-resolved photoemission (ARPES) and scanning tunneling microscopy (STM). We show a method to identify single and bilayer of graphene films by comparing characteristic features in electron reflectivity spectra in LEEM [3] to the π-band structure as revealed by ARPES. The structure of the underlying interface carbon layer is characterized using area-selective low energy electron diffraction and STM. Our study demonstrates that LEEM serves as a tool to accurately determine the local extent of graphene layers as well as the layer thickness, needed in understanding the high temperature growth process and the interface structure of graphene films on SiC, and in optimizing graphene growth conditions for large-scale uniformity.

References
[1] K. S. Novoselov, E. McCann, S. V. Morosov, V. Fal'ko, M. I. Katsnelson, U. Zeitler, D. Jiang, F. Schedin, A. K. Geim, 2005 *Nature* 438, 192: Y. Zhang, Y. W. Tan, H. L. Stormer, P. Kim, 2005 *Nature* 438, 201.
[2] T. Ohta, F. El Gabaly, A. Bostwick, J. L. McChesney, K. V. Emtsev, A. K. Schmid, Th. Seyller, K. Horn, E. Rotenberg, 2008 *New J. Physics* 10, 023034.
[3] H. Hibino, H. Kageshima, F. Maeda, M. Nagase, Y. Kobayashi, H. Yamaguchi, 2008 *Phys. Rev. B* 77, 075413.

Near-edge x-ray absorption fine structure investigation of graphene

D. Pacilé[1,4,5,*], M. Papagno[1], A. Fraile Rodríguez[2], M. Grioni[3], and L. Papagno[1],

C. Ö. Girit[4,5], J. C. Meyer[4,5], G. E. Begtrup[4,5] , and A. Zettl[4,5]

[1]*Istitut. Naz. di Fisica Nucleare (INFN) and Dip. di Fisica Universit`a della Calabria, 87036 Arcavacata di Rende, Cosenza, Italy*
[2]*Swiss Light Source, Paul Scherrer Institut, CH 5232 Villigen, Switzerland*
[3]*Institut de Physique des Nanostructures, Ecole Polytechnique Fédérale de Lausanne (EPFL), CH-1015 Lausanne, Switzerland*
[4]*Department of Physics, University of California, Berkeley, CA 94720, USA*
[5]*Materials Sciences Division, Lawrence Berkeley National Laboratory, Berkeley, CA 94720, USA*

*Email: dpacile@fis.unical.it

We report the near-edge x-ray absorption fine structure (NEXAFS) spectrum of a single layer of graphite (graphene) obtained by micromechanical cleavage of Highly Ordered Pyrolytic Graphite (HOPG) on a SiO2 substrate. We utilized a PhotoEmission Electron Microscope (PEEM) to separately study single- double- and few-layers graphene (FLG) samples. In single-layer graphene we observe a splitting of the π^* resonance and a clear signature of the predicted interlayer state. The NEXAFS data illustrate the rapid evolution of the electronic structure with the increased number of layers [1].
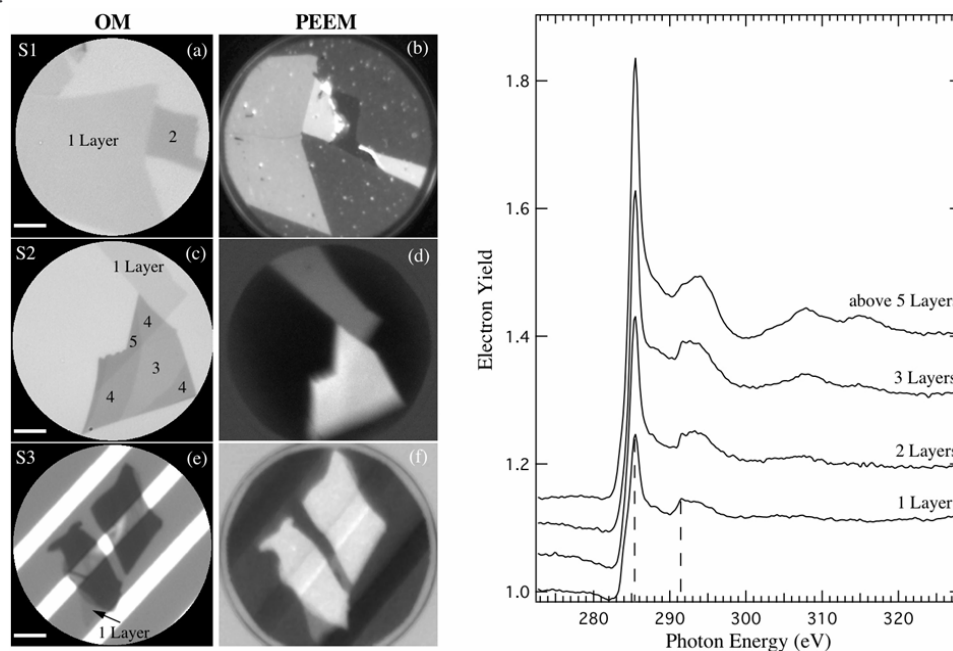
Fig.1 (left) OM images [(a), (c) and (e)] and PEEM ones [(b), (d) and (f)] of some selected samples (S1, S2 and S3). Scale bars are: 5 μm in (a) and (e); 10 μm in (c).
(right) C K-edge photoabsorption spectra of (from the bottom): graphene, bilayer graphene and FLG samples. Dashed lines show the C1s -π^* and C1s -σ^* transitions.

References
[1] D. Pacilé, M. Papagno, A. Fraile Rodríguez, M. Grioni, and L. Papagno, C. Ö. Girit, J. C. Meyer, G. E. Begtrup, and A. Zettl, Phys. Rev. Lett (2008) (accepted)

Using real-time observations to understand why the Au/W(110) system forms stripes at high temperature

J. de la Figuera[1,2], F. Léonard[3], N. C. Bartelt[3], R. Stumpf[3], and K. F. McCarty[3]

[1]*Instituto de Química-Física Rocasolano, CSIC, Madrid, Spain*
[2]*Universidad Autónoma de Madrid, Madrid, Spain*
[3]*Sandia National Laboratories, Livermore, CA 9455*

Email: juan.delafiguera@iqfr.csic.es

Ordered patterns sometimes spontaneously form on solid surfaces. In this work we study the remarkable example of Au on W(110): as first observed by Duden and Bauer[1, 2], submonolayers of Au on W(110) self-assemble into stripe patterns, which consist of monolayer-thick stripes of condensed-phase Au in coexistence with stripes of a Au adatom gas. Unlike other pattern-forming systems, the stripes in this system form along a particular crystallographic substrate direction, [1-10].

On solid surfaces, this kind of pattern is usually attributed to the competition between the short-range attractive interaction between atoms, leading to a phase-boundary energy, and a long-range repulsive interaction between boundaries, due to the difference in surface stress between the two phases. This repulsion is mediated by elastic deformations of the substrate. Determining whether these physics or other effects cause the pattern formation can be difficult using only static images of the self-assembling system.

Here we present a real-time study of how the Au/W(110) system forms stripes: by means of low energy electron microscopy, we have been able to follow the evolution of the pattern both with coverage and temperature[3]. Furthermore, we have been able to locate the pattern within the phase diagram of Au on W(110). The pattern appears close to the temperature where a transition to a homogeneous phase occurs (we call this temperature the order-disorder transition). We demonstrate that the amplitude of the pattern decreases steadily with increasing temperature and vanishes at the transition temperature. The modulation wavelength also decreases with temperature, depends quadratically on the reduced temperature, but remains finite (at 100 nm) at the transition temperature.

We have been able to reproduce the experimental results by means of a model that includes the following crucial experimental observations. First, the boundaries between the stripes become increasingly diffuse with increasing temperature. Second, both the monolayer island stripes and the areas between them change their local Au density as the total Au coverage changes.

By comparing our results with theoretical calculations of the stripe periodicity, we predict that this style of stripe patterns with nanometer scale should be common near two-dimensional critical points.

References
[1] T. Duden, Ph.D. thesis, Technischen Universitat Clausthal, 1996.
[2] E. Bauer, in The many facets of metal epitaxy, edited by D. A. King and D. P. Woodruff (Elsevier, Amsterdam,1997), Vol. 3, Chap. 2, p. 46.
[3] J. de la Figuera, F. Leonard, R. Stumpf, N. C. Bartelt, and K. F. McCarty, *Phys. Rev. Lett.* 100, 186102 (2008).

Elastic effects in adsorbate systems: Stress-Induced Pattern Formation

T. O. Menteş[1], A. Locatelli[1], L. Aballe[2], N. Stojić[3,4], M. A. Niño[1], N. Binggeli[5,4], M. Kiskinova[1], E. Bauer[6],

[1]*Sincrotrone Trieste S. C. p. A., Basovizza-Trieste 34012, Italy*
[2]*CELLS-ALBA Synchrotron Light Facility, 08193 Bellaterra, Barcelona, Spain*
[3]*SISSA, Via Beirut 2-4, Trieste 34014, Italy*
[4]*Theory @ Elettra Group, INFM-CNR Democritos, Trieste 34014, Italy*
[5]*Abdus Salam International Centre for Theoretical Physics, Strada Costiera 11, Trieste 34014, Italy*
[6]*Department of Physics, Arizona State University, Tempe, Arizona 85287-1504, USA*

Email: mentest@elettra.trieste.it

Recently, we have shown that small adsorbate islands tend to reduce the stress by elastic relaxations at the island boundaries [1]. In reality, the energy gain from such relaxations is in competition with the cost of forming boundaries. In general, competing long-range and short-range interactions may give rise to phase separation at length scales considerably above atomic distances. Indeed, the presence of mesoscopic patterns due to a balance between elastic (long-range) and adsorbate-adsorbate (short-range) interactions was predicted [2], almost in an identical fashion to the magnetic patterns expected from spin lattices with dipolar interactions [3].
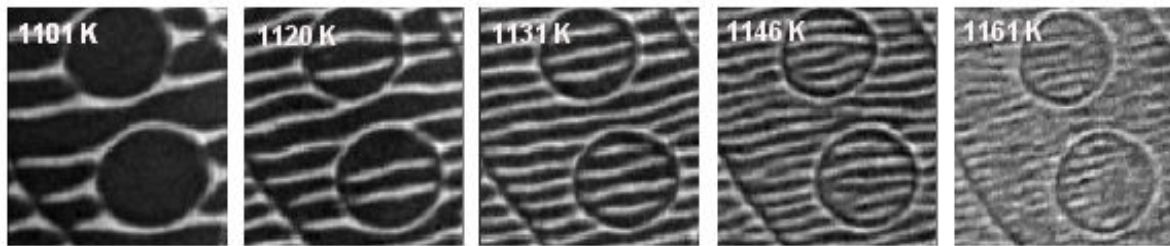

Figure. Alternating stripes of condensate and lattice gas phases of Pd on W(110) with increasing temperature. The size of the image is 1 µm. The circular patterns are atomic steps on the tungsten surface.

Along these lines, we report our observation of a stripe phase of submonolayer Pd on W(110) [4]. The alternating stripes of condensed and lattice gas regions of adsorbate atoms disorder at about 1170 K. We show that the evolution of the system with temperature follows a critical scaling similar to that of the striped patterns in the Ising spin lattice. Moreover, by measuring the low-energy electron diffraction intensity of the Pd lattice, we find that the actual condensate to lattice gas transition happens very close to but slightly above the stripe disordering temperature, in agreement with the scaling arguments.

References
[1] T. O. Menteş, N. Stojić, N. Binggeli, M. A. Niño, A. Locatelli, L. Aballe, M. Kiskinova, E. Bauer, 2008 *Phys. Rev. B* **77**, 155414.
[2] O. L. Alerhand, D. Vanderbilt, R. D. Meade, J. D. Joannapoulos, 1987 *Phys. Rev. Lett.* **61**, 1973.
[3] K. De'Bell, A. B. MacIsaac, J. P. Whitehead 2000 *Rev. Mod. Phys.* **72**, 225.
[4] T. O. Menteş, A. Locatelli, L. Aballe, E. Bauer, submitted.

Observing the kinetic pathways metal films use to de-wet substrates

Kevin F. McCarty[1], Yu Sato[2], Angela Saá[3], Juan de la Figuera[3,4], Benito Santos[3,4], Andreas Schmid[2], Konrad Thürmer[1], and Norman C. Bartelt[1]

[1]*Sandia National Laboratories, Livermore, CA*
[2]*Lawrence Berkeley National Laboratory, Berkeley, CA*
[3]*Universidad Autónoma de Madrid, Madrid Spain*
[4]*Instituto de Química-Física "Rocasolano", CSIC, Madrid Spain*

Email: mccarty@sandia.gov

Many film/substrate systems are unstable if the film uniformly covers the substrate. That is, the thermodynamically stable configuration is not a flat film but discrete, 3D islands. The area between the 3D islands exposes either bare substrate or a thin wetting layer. While low-temperature deposition can sometimes avoid 3D island formation, the films typically are quite rough on small length scales. Annealing can smooth these films if the kinetic processes that de-wet the film are slow compared to the smoothing processes.

For continuous films to de-wet, they must thin sufficiently in local regions to expose the bare substrate (or wetting layer). In other regions the film must thicken so 3D islands can form. Both the thinning and thickening processes would seem to require nucleating pits in film layers and nucleating new film layers, respectively. Yet these obvious pathways seem unlikely since their nucleation processes should have substantial energy barriers.

The dynamic view of surface evolution provided by LEEM can provide the necessary clues to understand de-wetting. We have previously used this approach to identify a kinetic pathway that short circuits high-energy barrier processes in film thickening [1]. Here we gain additional insight, particularly into how thinning occurs, by studying Cr on W(110). Like in Fe/W(110) [2], the 3D islands in this system are unidirectional stripes, which greatly simplifies observing the de-wetting mechanism.

Our microscopic observations reveal that de-wetting occurs by atomic film steps in adjacent regions moving in different directions relative to the fixed substrate steps. First, a section of an atomic film step advances (downhill), making this local region thicker, and, therefore, more stable than surrounding regions. This thicker region then draws material from adjacent areas where steps retract (uphill). These instabilities grow and eventually form trenches that reach the wetting layer. With time, the Cr stripes between the trenches become continuously narrower and thicker. We believe that the observed de-wetting mechanism, involving the cooperative motion of film steps, will be operative in other de-wetting film/substrate systems.

References
[1] W. L. Ling et al., Surf. Sci. 570, L297 (2004).
[2] R. Zdyb, A. Pavlovska, M. Jalochowski, E. Bauer, Surf. Sci. 600, p.1586 (2006).

A PEEM ThEEM-study of Ba/Sc Thin Film and Porous Metal Thermionic Cathodes

Joel M. Vaughn[1] , Keith Jamison[2] and Martin E. Kordesch[1]

[1]*Department of Physics and Astronomy, Ohio University, Athens Ohio USA 45701-2979*
[2]*Nanohmics, Inc., Austin, Texas USA 78741*

Email: kordesch@ohio.edu

In order to understand the effect of Sc- and Ba- oxides on the emissivity of high current density cathodes we have imaged thin films of scandium oxide and barium oxide on tungsten foils using photoelectron emission microscopy and thermionic emission microscopy. In order to understand the re-supply mechanism of porous metal and reservoir cathodes using these materials we have imaged diffusion through and onto porous titanium and tungsten media with patterned thin films of Sc on the surface.

For thermionic emission studies arrays of 100 um X 100 um squares of scandium and 25 um x 25 um squares of barium, 200 nm thick, were sputter deposited onto 50 um thick sheets of tungsten foil. The barium oxide squares emit below 875 K, and diffuse over the scandium, also at temperatures below 875 K. Thermionic emission from scandium oxide squares is observed at temperatures significantly higher than 875 K. Failure of the barium oxide film cathode is through barium desorption. At higher temperatures, where thermionic emission from scandium oxide squares is observed; un-oxidized scandium metal diffuses into the spaces between the scandium oxide squares, and mixes with Ba/Ba-oxide. Emission failure is due to a poisoning mechanism. AES spectra show that the Sc does not desorb. In test of combined Sc + Ba squares, the overlapped areas emit at lower temperature than barium oxide alone. The presence of scandium oxide seems to enhance the diffusion of barium oxide.

In the diffusion studies arrays of 100 um x 100 um squares of scandium, 200 nm thick, were sputtered deposited onto porous tungsten on the imaged side and exposed to air as before. The opposite side of the sample was either sputter deposited with Ba or Sc or it was filled with Ba- or Sc- Oxide powders. As the samples were heated metals diffused through the pores. Pore sizes on the order of c. 100 microns allowed the metals from the back side of the cathode to pass through in a gaseous phase without being deposited onto the surface. Smaller pores resulted in a slower diffusion, and more metal was deposited onto the surface.

Smaller grain size and pores, though more apt to fail due to poisoning and cloging, result in a more evenly distributed metal deposition onto the cathode surface. The transport of the Ba-Sc to the surface and surface deposition depends on pore size and pore distribution. Further extension of the lifetime of scandate cathodes will depend on controlled cathode material porosity.

Step Contrast Reversal in LEEM during Pb Deposition on W(110)

T. Yasue[1], R. Amakawa[1], H. Shimizu[1], A. Nakaguchi[1], E. Bauer[2] and T. Koshikawa[1]

[1]*Fundamental Electronics Research Institute, Osaka Electro-Communication Univ.,*
18-8 Hatsu-cho, Neyagawa, Osaka 572-8530, Japan
[2]*Department of Physics and Astronomy, Arizona State Univ., Tempe, AZ 85287, USA*

Email: yasue@isc.osakac.ac.jp

Step contrast in LEEM is understood by the interference of electrons reflected from upper and lower terraces, and steps appear darker than surrounding terraces in general [1]. In the present paper, we will show anomalous behavior of step contrast in LEEM during the growth of Pb on W(110) surface with in monolayer regime and discuss the step contrast mechanism.

Figure 1 shows LEEM images during growth of Pb on W(110) surface. Monoatomic steps appear dark on the clean W(110) surface as shown in (a). Steps become brighter than surrounding terraces at around 0.06ML as shown (b). With further deposition of Pb, steps are observed dark again above about 0.45ML as shown (c). In order to understand this anomalous step contrast reversal, the intensity along steps and terraces were continuously measured during deposition. Both intensities weaken with increase coverage up to around 0.4ML. The initial decrease of the intensity on the terrace is explained by the presence of 2D Pb gas on the surface. The relative intensity decrease of steps is smaller than that of terrace and this induces the anomalous step contrast reversal. The reason of slow intensity decrease along steps is considered that the density of 2D Pb gas is much smaller than that on the terraces. This means that the repulsive interaction acts at steps to Pb gas. With increasing coverage beyond 2D gas limit, the condensation and crystallization of Pb layer starts, which could be confirmed by appearance of LEED spots from the Pb layer. Then both intensities along steps and on terraces recover and the intensity along steps becomes smaller relative to that on terraces which corresponds to the step contrast reversal from bright to dark.

The details of the results will be presented at the conference.

Fig.1: step contrast change in Pb/W(110).

References

[1] W.F. Chung and M.S. Altman, Ultramicroscopy 74 (1998) 237.

Fourier Optics Model Calculation of LEEM Step Contrast

A.B. Pang[1], Th. Müller[2], M.S. Altman[1], Ernst Bauer[2]

[1]*Department of Physics, Hong Kong University of Science and Technology*
Clear Water Bay, Kowloon, Hong Kong, P.R.China
[2]*Physikalishes Institut, Technische Universität Clausthal, Leibnizstrasse 4*
D-38678 Clausthal-Zellerfeld, Germany

Email: phaltman@ust.hk

Step contrast in low energy electron microscopy (LEEM) derives from the interference of the electron waves that are reflected from terraces on opposing sides of surface steps. The phase shift that gives rise to this interference phenomenon is proportional to the ratio of the path length difference, i.e. twice the step height, and the electron wavelength. This elementary description has been confirmed by a wave-optical model calculation of the interference between the Fresnel diffracted waves that are produced by an equivalent pair of suitably shifted straight-edge apertures [1,2]. Model predictions also exhibit effects that are analogous to the experimentally observed dependence of step contrast on incident electron energy and defocus. Although the detrimental intrinsic effect of electron beam coherence, defined by energy spread and source extension, were shown realistically, objective lens aberrations and diffraction error were treated only in an ad-hoc way by Gaussian convolution. In the present work, the Fourier optics calculation approach [3,4] that was developed for high energy electron microscopy has been adapted to evaluate LEEM step contrast. The advantage of this approach is that aberrations and diffraction error can be handled properly using aberration coefficients and aperture angle appropriate for LEEM, in addition to treating beam coherence and defocus. This leads to model predictions that may be compared quantitatively to experimental observations. Besides evaluating contrast that arises from phase objects such as surface steps, the Fourier optics method is equally well suited for treating amplitude objects that produce what is commonly called diffraction contrast.

References
[1] W.F. Chung and M.S. Altman, Ultramicroscopy **74**, 237 (1998).
[2] M.S. Altman, W.F. Chung, C.H. Liu, Surf. Rev. Lett. **5**, 1143 (1998).
[3] Th. Müller, Diplomarbeit, TU Clausthal (1995).
[4] Oker K. Ersoy, *Diffraction, Fourier Optics and Imaging* (Wiley, Hoboken, 2007).